Journal Name

ARTICLE

Photochemical investigation of cyanoazobenzene derivatives as components of artificial supramolecular pumps

Lorenzo Casimiro,[a,b,e] Jessica Groppi,[b,c,e] Massimo Baroncini,[b,c,d] Marcello La Rosa,[b,c] Alberto Credi,[b,c,d] and Serena Silvi*[a,b]

Among the plethora of photochromes reported so far, azobenzene has been proven to be the most suitable photoswitch for molecular systems and materials, due to its highly efficient and clean *E-Z* photoisomerization. Here we report two ammonium-based molecular axles bearing one or two *p*-cyanoazobenzene units at the extremities, able to form pseudorotaxanes with a crown ether macrocycle. The photochemistry of these compounds was studied in the isolated forms and in the pseudorotaxanes, showing that the functionalization speeds up the threading process without affecting the photochemical properties of the system. These results suggest that the investigated pseudorotaxanes can form the basis of new prototypes of artificial molecular-level pumps.

Introduction

Photochromic compounds are widely exploited in the development of functional molecular systems and materials,[1,2,3] as their switching abilities can be used to modulate the properties of the systems.[4,5] The *E-Z* photoisomerization of azobenzene and its derivatives has been known for more than 80 years[6] and is highly useful in the frame of the realization of photocontrollable molecular species.[7] The photoisomerization of azobenzene is efficient and reversible, and causes relevant changes in its shape and properties: notably, the *E* isomer is planar and apolar, whereas the *Z* isomer is non-planar and polar.[8] The utility of these features in several areas – from chemistry[9] to biology,[5] medicine[10] and material science[11] – is well documented.

Azobenzene derivatives have been largely employed in supramolecular chemistry,[12] for example in host-guest systems, wherein either the photoisomerization is used to control the properties of the supramolecular adducts,[13] or the other way round, namely, the formation of non-covalent interactions affects the photoreactivity of the molecular switch.[14] Azobenzenes have also been adopted as functional elements in the design of molecular machines, because the large shape changes associated to isomerization can be exploited, e.g., to afford large amplitude motions,[15,16] or to exert a kinetic control over dynamic processes.[17,18]
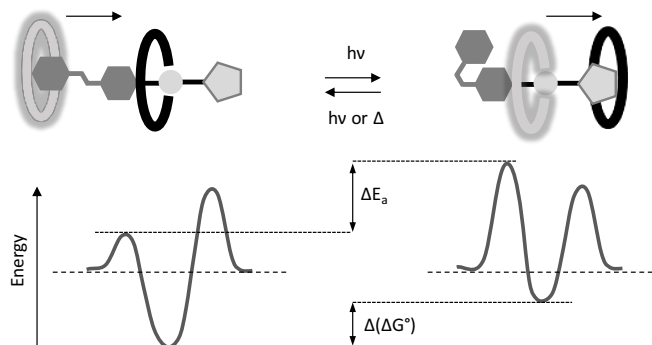

Figure 1. Schematic representation (top) and simplified potential energy curves (bottom) for the operation of an artificial molecular pump triggered by light.

We recently reported an artificial molecular pump based on a pseudorotaxane,[19] wherein an azobenzene end group is used both as thermodynamic and kinetic control element (Figure 1).[20,21] The molecular motor is composed of an ammonium unit derivatized with a (*p*-methyl)azobenzene on one side and a cyclopentyl moiety on the other side as the axle component, and a 2,3-dinaphtho[24]crown-8 ether as the molecular ring. The two molecules self-assemble spontaneously by virtue of hydrogen bonding interactions between the secondary ammonium station and the crown ether. This supramolecular system is characterized by two main features: i) the hindrance of the cyclopentyl unit for the

a. *Dipartimento di Chimica "G. Ciamician", Università di Bologna, via Selmi 2, 40126 Bologna, Italy. E-mail: serena.silvi@unibo.it*
b. *CLAN-Center for Light Activated Nanostructures, Università di Bologna and Consiglio Nazionale delle Ricerche, via Gobetti 101, 40129 Bologna, Italy.*
c. *Dipartimento di Scienze e Tecnologie Agro-alimentari, Università di Bologna, viale Fanin 50, 40127 Bologna, Italy*
d. *Istituto per la Sintesi Organica e la Fotoreattività, Consiglio Nazionale delle Ricerche, via Gobetti 101, 40129 Bologna, Italy.*
e. *These authors contributed equally to the paper*

threading of the macrocycle is in-between the ones of *E* and *Z* azobenzene, ii) the stability of the pseudorotaxane decreases upon isomerization of the azobenzene from *E* to *Z* (Figure 1). As a result of this design, the pseudorotaxane can thread and dethread unidirectionally under light irradiation. The operation of the molecular motor can be summarized as follows (Figure 1): a) unidirectional threading of the ring from the *E*-azobenzene extremity; b) photoisomerization of the azobenzene from *E* to *Z*; c) unidirectional dethreading from the cyclopentyl extremity; d) thermal- or photochemical isomerization of the azobenzene from *Z* back to *E*.

In summary, the dual role of the azobenzene, when isomerized from *E* to *Z* configuration, is to destabilize the supramolecular complex and prevent the dethreading of the macrocycle from the azobenzene side. As the same photons cause *E→Z* and *Z→E* isomerization, the system can repeat its operation cycle autonomously, as long as the energy source is available. With the aim of improving the efficiency of this kind of molecular motor, we are investigating novel axle components wherein the azobenzene ring is functionalized with proper substituents. Specifically, our efforts are devoted to increasing both the stability difference between the *E* and *Z* pseudorotaxanes and the selectivity for the threading and dethreading directions, while avoiding detrimental consequences on the photochemical properties of the switch.

Functionalized azobenzenes can be classified in three main categories, depending on how the photochemical properties are affected by the substituents:[8,22] amino-azobenzenes, pseudo-stilbenes and azobenzene-type. We are focusing on the latter class of derivatives, which maintain the photochemical and photophysical features of azobenzene. Therefore we have synthesized two axle components in which a secondary ammonium unit is functionalized with one or two (*p*-cyano)azobenzene extremities (Figure 2). The aim of our study is a thorough photochemical characterization of the molecular axle **1**H^{+}, of its symmetric model compound **2**H^{+}, and of the corresponding pseudorotaxanes with macrocycle **3**. In the frame of the exploitation of these axles as molecular motor components, a preliminary investigation on the thermodynamic and kinetic parameters of the *E*-**1**H^{+}⊂**3** pseudorotaxane is also undertaken.
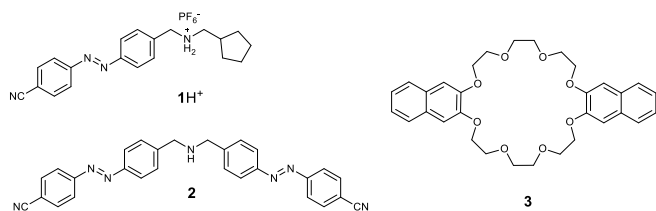

Figure 2. Molecular structures of the investigated compounds.

Results and discussion

All the compounds were characterized in CH$_2$Cl$_2$, which is the solvent of choice for the operation of the molecular pump.

The photophysical and photochemical data are gathered in Table 1.

Compound **1**H^{+} was obtained by Mill's coupling of 4-nitrosobenzonitrile with 4-{[(cyclopentylmethyl)amino]methyl} aniline in acetic acid, followed by anion exchange with NH$_4$PF$_6$. Compound **1**H^{+} can be fully deprotonated upon addition of 1 equivalent of tributylamine. Compound **2** was analogously synthesized by Mill's coupling of 4-nitrosobenzonitrile with bis(4-aminobenzyl)amine. Given the very poor solubility of the acetate salt of **2** in most solvents, it was decided to isolate it as the free amine. Compound **2** could be protonated at the concentration used for UV-Vis spectroscopic investigations (below 10^{−4} M) upon addition of 1 equivalent of triflic acid.

Table 1. Photophysical and photochemical data of the investigated compounds.

Compound	λ_{max}/ϵ (M^{-1}cm^{-1})[a]	$\Phi_{E\to Z}$[b] (365 nm)	$\Phi_{Z\to E}$[c] (436 nm)	$k_{Z\to E}$ (s^{-1})[d]
1	338/30000 451/940	0.09	0.38	9.4×10^{-6}
1H[+]	323/31000 451/650	0.02	0.41	3.6×10^{-6}
1H[+]⊂**3**	323/37000 451/650	0.03	0.40	9.7×10^{-6}
2	339/42000 453/1300	0.04	0.32	7.8×10^{-6}
2H[+]	326/44000 453/990	0.01	0.23	3.8×10^{-5}
2H[+]⊂**3**	323/51000 453/990	0.02	0.25	1.3×10^{-5}

[a] Wavelength and molar coefficient of the π-π* and n-π* absorption band maxima; [b] quantum yield of *E→Z* photoisomerization upon irradiation at 365 nm; [c] quantum yield of *Z→E* photoisomerization upon irradiation at 436 nm; [d] rate constant of thermal *Z→E* isomerization at room temperature.

The absorption spectra of the two ammonium salts **1**H^{+} and **2**H^{+} show the typical features of azobenzene derivatives, with an intense and slightly structured π-π* band in the UV, and a weaker and broader n-π* band in the visible, around 450 nm. In the absorption spectra of the deprotonated compounds **1** and **2** the π-π* band is shifted toward lower energies, whereas the n-π* band is almost unaffected with respect to the protonated compounds (Figure 3).

All the compounds were isomerized from the *E* to the *Z* configuration by irradiation with UV light (365 nm); back isomerization was accomplished both photochemically, i.e., by irradiation with visible light (436 nm), or thermally. Upon irradiation of **1** and **2** at 365 nm the typical absorption changes associated to *E*-*Z* isomerization are observed:[8] namely, the π-π* band is shifted to higher energies and becomes less intense, whereas both the energy and the intensity of the n-π* band increase (Figures 3 and 4). The percentage of *E* to *Z* conversion at the photostationary state (PSS) is around 90%, with a quantum yield of 0.09 and 0.04 for **1** and **2**, respectively.[8]

It is worth noting that compound **2**, having the two units in *EE* configuration, can evolve under irradiation towards both the *EZ* and *ZZ* ~~isomers contains two azobenzene units, which can lead, in principle, to three different isomers: *ZZ, EE* and *EZ*~~. From a careful analysis of the absorption changes associated to the irradiation experiment, indeed, only one family of isosbestic points can be identified, which is maintained along the irradiation. This observation suggests that the two

photochromic units behave independently, and in our conditions it is not possible to distinguish the different isomers.[20] Therefore in the forthcoming discussion we will refer to the percentage of E and Z isomers of the azobenzene units in the ensemble solution. Indeed, the fact that the quantum yield of photoreaction of **2** is around half of the quantum yield of compound **1** is consistent with the presence of two azobenzene units for each molecule of **2**. The quantum yields for the back photoreactions are affected by a larger error, due to the relatively low absorbance of the Z form at the irradiation wavelength, and the presence of a significant amount of E species. Nevertheless the quantum yield of compound **2** is lower than that of compound **1**, as expected. Isomerization from Z to E was accomplished also thermally: by leaving the photolyzed solution in the dark, the initial spectra of the E isomers are obtained after a few days (Table 1, Figure 4).
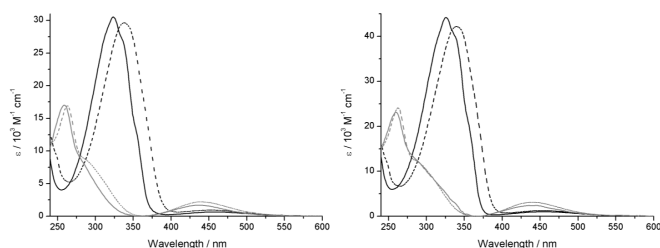

Figure 3. Absorption spectra of compounds **1** (left) and **2** (right). Black lines: E isomers; grey lines: Z isomers; solid lines: protonated compounds; dashed lines: neutral compounds.
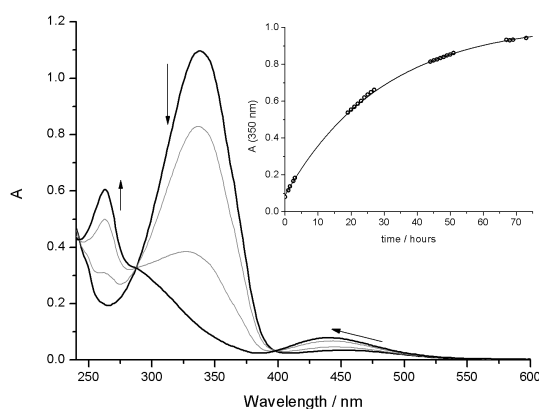

Figure 4: Absorption spectra of a 3.7×10^{-6} M solution of **1** upon irradiation at 365 nm. The inset shows the absorption changes at 350 nm upon $Z{\to}E$ thermal isomerization (white circles) and the fitting of the data with a first order reaction (solid line).

The $E{\to}Z$ isomerization of the protonated salts **1**H$^+$ and **2**H$^+$ caused by irradiation at 365 nm, is accompanied by spectroscopic changes similar to those of the deprotonated compounds (Figure 3). However, the percentage of photoconversion is lower, around 80% for **1**H$^+$ and below 50% for **2**H$^+$, and also the quantum yields are much smaller with respect to the non-protonated molecules (and to parent azobenzene photochromes). Back $Z{\to}E$ isomerization could be

accomplished upon visible irradiation and the quantum yields were estimated (Table 1). Upon leaving the systems in the dark a complete recovery of the E isomers was obtained in a few days, in analogy with the non-protonated compounds.

Understanding the photochromic behaviour of **1**H$^+$ and **2**H$^+$ is less straightforward than that of **1** and **2**. In particular,we noticed that the irradiation of a solution at a given wavelength, either in successive steps or in a single session for the same total illumination time, leads to different PSS compositions. A contribution of the Z to E thermal reaction can be excluded, because this process is too slow on the time scale of the irradiation. We must therefore hypothesize that some kind of time-dependent process takes place while the solution is spectroscopically analyzed between two consecutive irradiations, such as, for example, molecular aggregation. This is not surprising, considering the low solubility of these compounds. These phenomena could also be responsible for the low quantum yields of the protonated compounds.

It is well known[23] that secondary ammonium salts are good guests for crown ethers, with association constants exceeding 10^6 M^{-1} in apolar solvents.[24] In particular, the investigated compounds are designed to play the role of axle components in pseudorotaxane systems, in which the macrocycle is the 2,3-dinaphtho[24]crown-8 ether ring **3**.[25]

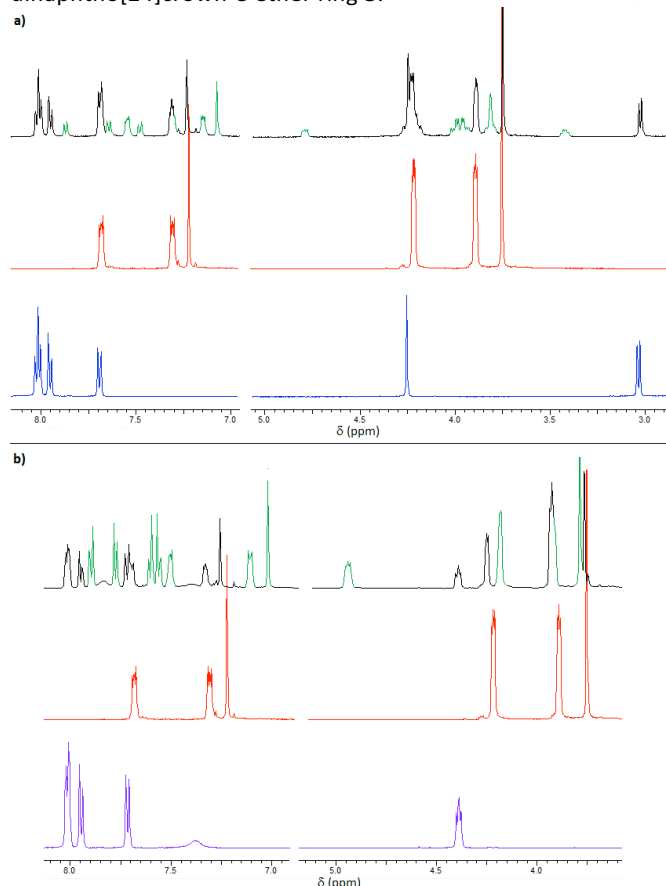**Figure 5**. ^{1}H-NMR spectra (500 MHz, 298 K, CD$_3$CN) of 3 mM solutions of free compounds and of an equimolar mixture of the components. a) Blue line: **1**H$^+$; red line: **3**; black line: 1:1 mixture solution, the peaks of the complex are highlighted in green. b) Purple line: **2**H$^+$; red line: **3**; black line: 1:1 mixture solution, the peaks of the complex are highlighted in green.

The formation of pseudorotaxanes between axles $1H^+$ and $2H^+$ and the macrocycle **3** was confirmed by ^{1}H-NMR spectroscopy. As the solubility of the axles in dichloromethane does not enable the preparation of mM solutions, the NMR experiments were performed in acetonitrile. Figure 5a shows the ^{1}H-NMR spectrum of a 1:1 mixture of compounds $1H^+$ and **3** in CD$_3$CN at 298 K, together with the spectra of the individual components. The spectrum of the mixture presents the characteristic peaks associated with the formation of complex $1H^+⊂3$ in addition to the signals of the free components. Figure 5b shows the ^{1}H-NMR spectra of $2H^+$, **3**, and their 1:1 mixture in CD$_3$CN at 298 K. In order to obtain the protonated form of compound **2** for the NMR complexation experiments, the axle was suspended in CD$_3$CN and 1 equivalent of deuterated triflic acid was added, followed by addition of macrocycle **3**. Also in this case, the ^{1}H-NMR spectrum of the mixture is characterized by the typical peaks attributed to complex $2H^+⊂3$. The results obtained are consistent with reported data related to the formation of pseudorotaxanes in which a crown ether is located around an ammonium-type axle, and they indicate that the threading/dethreading processes are slow on the ^{1}H-NMR timescale.[20,21]
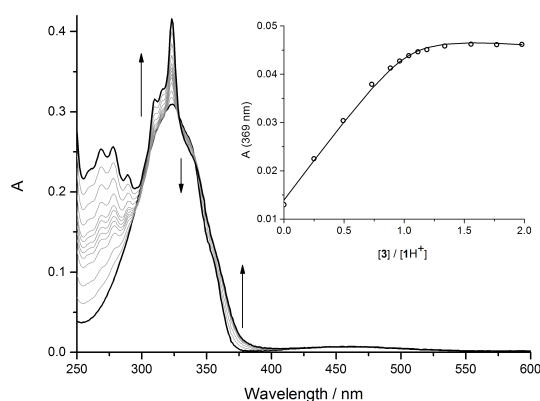

Figure 6. Absorption spectra of a $1.1×10^{-6}$ M solution of $1H^+$ upon titration with **3**. The inset shows the absorption changes at 369 nm (white circles) and the fitting of the data (solid line).

UV-Vis spectroscopic titrations were performed to determine the association constants of the pseudorotaxanes in CH$_2$Cl$_2$. A solution of either $1H^+$ or $2H^+$ was titrated with **3**: in both cases, small absorption changes are observed in the 340-550 nm region, in which the crown ether does not absorb (Figure 6). The corresponding titration curve reaches saturation at ca. 1 equivalent of **3**, suggesting the formation of a 1:1 complex and in agreement with the NMR data.

Macrocycle **3** is characterized by an intense luminescence, which is partially quenched by the guest molecules, most likely for energy and/or electron transfer processes.[19] The association constants determined from absorption titrations are $3.7×10^6$ M^{-1} for $1H^+⊂3$ and $3×10^5$ M^{-1} for $2H^+⊂3$, and are in line with those obtained for related compounds.[19,24] Despite the high similarity of the recognition sites, the two association constants differ for more than one order of magnitude. Such a difference may be ascribed to the different counterions of $1H^+$

and $2H^+$, which are respectively hexafluorophosphate and triflate. It is well known[26] that, for this type of compounds, ion pairing competes with threading in apolar solvents and thus can influence the apparent stability constants measured with UV-Vis spectroscopic techniques, which cannot distinguish between the free and ion-paired guests. The smaller association constant of $2H^+⊂3$ can be rationalized because triflate is a more coordinating ion than hexafluorophosphate.[26,27,28] Nevertheless, the complex is stable enough to consider it for our experiments.

The threading kinetics of compound $1H^+$ with **3** was also investigated: upon mixing $1H^+$ and **3** in stoichiometric ratio, the emission decrease in time of the crown ether can be followed (Figure 7).‡ The kinetic traces were fitted with a model consisting of a bimolecular threading and first-order dethreading processes (mixed order reaction, eq. 1):
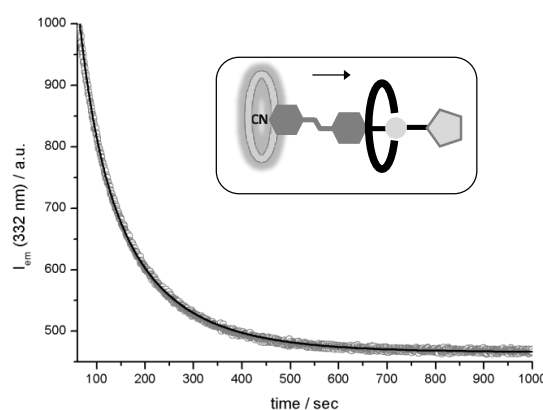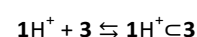
$$1H^+ + 3 ⇆ 1H^+⊂3$$

Figure 7. Emission changes at 332 nm observed as a function of time after mixing two equimolar solutions of **3** and $1H^+$ ($2.3×10^{-6}$ M). The solid line is the fitting of the data with a mixed order model (see text for details). The cartoon is a schematic representation of the undirectional threading process of crown **3** from the (p-cyano)azobenzene extremity of $1H^+$.

The value of the equilibrium constant for the reaction was fixed in the model at the measured value of $3.7×10^6$ M^{-1}. The rate constant for the threading process determined from the fitting of the data is $1.3×10^3$ M^{-1} s^{-1}. In principle, threading of the macrocycle can take place from the two different sides of the axle, i.e., by passing over the cyanoazobenzene moiety or the cyclopentyl unit. The rate constant for the latter process, as determined in previous investigations on a model symmetric ammonium axle with two cyclopentyl end groups, is 2.2 M^{-1} s^{-1}.[19] A comparison of these values suggests that the association between the two molecular components occurs through the azobenzene side.

It is worth noting that for the parent molecular pump reported in the literature,[19] wherein the azobenzene has a methyl group in the *para* position, the threading rate constant is 54 M^{-1} s^{-1}, i.e., more than two orders of magnitude slower with respect to the present pseudorotaxane. We could ascribe such a difference to the larger steric hindrance exerted by the

methyl group with respect to the linear cyano substituent; moreover, as the CN group has a large dipole moment, electronic effects cannot be excluded. This is a relevant result for the improvement of the operation of the molecular pump, in particular regarding the selectivity for the two different threading sides: the larger the difference in the threading rate, the larger the directional selectivity. Moreover the kinetic parameters affect the overall efficiency of the operation cycle.

The photochemical behaviour of $1H^+ \subset 3$ and $2H^+ \subset 3$ was investigated by irradiating solutions of axle and ring components in 1:1.5 ratio: at the typical concentrations of the photochemical experiments (around 10^{-5} M) more than 95% of $1H^+$ and at least 80% of $2H^+$ are complexed. Upon irradiation at 365 nm, where only the guests absorb, $E \rightarrow Z$ isomerization was accomplished with quantum yields similar to those measured for the free guests. Interestingly, the erratic photochemical behaviour of the protonated axles (vide supra) was no longer observed in the presence of 3, and stable and reproducible photostationary mixtures could be obtained. The conversion percentage at the PSS was around 80% for $1H^+ \subset 3$ and 70% for $2H^+ \subset 3$. The $Z \rightarrow E$ reaction was also observed in the complexes, both in the dark and upon irradiation at 436 nm (Table 1), again with kinetic parameters in line with those of the free axles.

Thus, we can conclude that the presence of the macrocyclic host around the ammonium center not only has almost no effect on the photochemical parameters of the azobenzene unit, in analogy with related systems,[19] but also removes reproducibility issues, most likely by favouring the solubilisation of the cationic guests in apolar solvents.

Conclusions

We have reported the photochemical investigation of two molecular components, comprising a secondary ammonium recognition site and either one or two (*p*-cyano)azobenzene moieties, which can form the basis of a light-driven molecular pump.[19] The two axle molecules, in their protonated and deprotonated forms, were characterized and their photochemical and thermal isomerization processes were investigated. In dichloromethane both ammonium salts form stable complexes with the 2,3-dinaphtho[24]crown-8 ether ring 3, a fact that removes some solubility issues observed for the free axles.

The ability of the nonsymmetric guest $1H^+$ to self-assemble efficiently with its host, combined with a valuable photoreactivity, confirms that the design employed is suitable for the development of light-driven supramolecular motors. In particular the fast threading kinetics, which is the most significant difference with respect to the first prototype,[19] could prove useful to increase the efficiency of the machine and reduce its cycle time.

In order to exploit our original design for developing molecular pumps with better performance and/or ability to perform tasks, the components of the first prototype need to be modified while maintaining the fundamental requirements of its operation mechanism. In this regard, structural tweaks

aimed at fine-tuning the thermodynamic and kinetic parameters associated with the threading-dethreading movements are of the utmost importance. Any modifications on the photochromic unit, however, must guarantee that its photochemical properties are preserved. Further investigations along this direction are underway in our laboratory.

Experimental

Materials and Characterization Methods

4-{[(cyclopentylmethyl)amino]methyl}aniline[21], bis(4-aminobenzyl)amine[29] and compound **3**[30] were synthesized according to previously published procedures. Commercially available compounds were reagent grade quality and were used without further purification. Solvents were dried according to literature procedures. ^{1}H and ^{13}C NMR spectra were recorded at 298 K with a Varian Mercury 400. All chemical shifts are reported using the δ scale and all coupling constants (*J*) are expressed in Hertz (Hz).

4-nitrosobenzonitrile. 4-aminobenzonitrile (2 g, 17 mmol) was dissolved in dichloromethane (60 ml) and added to a solution of Oxone (20 g, 65 mmol) in water (210 ml) to obtain a biphasic solution. The mixture was stirred vigorously. The organic phase became green after 15 minutes. The reaction was monitored until complete disappearance of the starting aniline. The aqueous layer was removed and the organic layer was washed with HCl 10% (100 ml), NaHCO$_3$ (sat.) (100 ml) and Brine (100 ml). The organic layer was dried over Na$_2$SO$_4$ and the solvent was removed to obtain a yellow solid. The product was purified by vapor current distillation, followed by recrystallisation from ethanol. The product was a yellow solid obtained in 70% yield (1.57 g). ^{1}H-NMR (400 MHz, d$_6$-DMSO): δ 8.27 (d, *J* = 8.2 Hz, 2H), 8.09 (d, *J* = 8.2 Hz, 2H). ^{13}C-NMR (400 MHz, d$_6$-DMSO): δ 162.9; 134.7; 120.8; 117.8; 117.7.

E-N-(4-((4-cyanophenyl)diazenyl)benzyl)-1-cyclopentylmethanamine (1H·PF$_6$). To a solution of 4-{[(cyclopentylmethyl)amino]methyl}aniline (200 mg, 1 mmol) in acetic acid (10 ml), 4-nitrosobenzonitrile (155 mg, 1.1 mmol) was added and the mixture was left stirring overnight at room temperature. The orange precipitate was filtered, washed with ethyl ether, and dissolved in water with a few drops of acetone. NH$_4$PF$_6$ was added to the solution to precipitate the hexafluorophosphate salt. The precipitate was filtered, washed with water, and dried under vacuum. The product was an orange solid obtained in 75% yield (348 mg). ^{1}H-NMR (400 MHz; CD$_3$CN): δ 8.03-8.00 (m, 4H), 7.95 (d, *J* = 8.4 Hz, 2H), 7.69 (d, *J* = 8.4 Hz, 2H), 4.26 (s, 2H), 3.05 (d, *J* = 7.5 Hz, 2H), 2.19 (m, 1H), 1.84 (m, 2H), 1.67-1.59 (m, 4H), 1.25 (m, 2H). ^{13}C-NMR (400 MHz, d6-DMSO): δ 153.8; 151.8; 136.3; 133.9; 131.3; 123.2; 123.1; 118.3; 113.6; 51.7; 50.1; 36.4; 30.1; 24.6.

4,4'-((1E,1'E)-((azanediylbis(methylene))bis(4,1-phenylene))bis(diazene-2,1-diyl))dibenzonitrile (2). To a solution of bis(4-aminobenzyl)amine (340 mg, 1.5 mmol) in acetic acid (15 ml), 4-nitrosobenzonitrile (462 mg, 3.5 mmol) was added and the mixture was left overnight stirring at room temperature. The reaction was quenched with NaHCO$_3$ (sat.)

until pH 7 was reached and the product was extracted with dichloromethane (100 ml). The organic layer was dried over Na_2SO_4 and the solvent removed. The solid was triturated with diethyl ether. The product was an orange solid obtained in 50% yield (341 mg). ^{1}H-NMR (400 MHz; d_6-DMSO): δ 8.08 (d, *J* = 8.5 Hz, 4H), 8.01 (d, *J* = 8.5 Hz, 4H), 7.94 (d, *J* = 7.8 Hz, 4H), 7.65 (d, *J* = 7.8 Hz, 4H), 3.91 (s, 4H). ^{13}C-NMR (400 MHz, d_6-DMSO): 154.0; 150.9; 133.8; 129.3; 123.1; 122.9; 118.4; 113.2; 109.5; 39.5**.**

Uv-Vis absorption and emission spectroscopy

All spectroscopic measurements were performed on air-equilibrated CH_2Cl_2 (Uvasol) solutions at room temperature. Quartz cuvettes with a 1 cm path length were used. UV-vis spectra were recorded with Varian Cary 300 and Varian Cary 50 Bio spectrophotometers. Emission spectra were recorded on a Varian Cary Eclipse fluorescence spectrometer. Spectrophotometric titrations were performed adding a concentrated solution of the host to a more diluted solution of the guest. The binding thermodynamic constants were obtained by fitting the absorbance changes with software SPECFIT, according to a 1:1 binding model. Threading kinetics were investigated monitoring the luminesce quenching of the host upon addition of the guest. Rate constants were obtained by fitting with software SPECFIT, according to a mixed order (second order threading – first order dethreading) kinetic model.

Irradiation experiments

Irradiation experiments were performed on air-equilibrated solutions, thoroughly stirred, at room temperature. A Hanau Q400 mercury medium pressure lamp (150 W) was used. The desired wavelength of irradiation (365 nm or 436 nm) was selected using an appropriate interference filter. The number of incident photons was determined by ferroxalate actinometry in its microversion.[31] Photoisomerization quantum yields were calculated following the absorbance changes on the π-π* band, within low conversion percentages (<10%).

Conflicts of interest

There are no conflicts to declare.

Acknowledgements

Notes and references

‡ The kinetics of threading of the symmetric axle **2**H^{+} in **3** was not investigated, as the triflate counterion could affect also the rate of the reaction and all the model compounds and related systems reported in the literature are hexafluorophosphate salts.

1   X. Yao, T. Li, J. Wang, X. Ma and He Tian, *Adv. Optical Mater.*, 2016, **4**, 1322.
2   D. Bléger and S. Hecht, *Angew. Chem. Int.Ed.*, 2015, **54**, 11338.
3   A. Fihey, A. Perrier, W. R. Browne and D. Jacquemin, *Chem. Soc. Rev.*, 2015, **44**, 3719.
4   C. L. Jones, A. J. Tansell and T. L. Easun, *J. Mater. Chem. A*, 2016, **4**, 6714.
5   A. A. Beharry and G. A. Woolley, *Chem. Soc. Rev.*, 2011, **40**, 4422.
6   E. Mitscherlich, *Ann. Pharm.*, 1834, **12**, 311.
7   M. Baroncini, G. Ragazzon, S. Silvi, M. Venturi and A. Credi, *Pure Appl. Chem.*, 2015,**87**, 537.
8   H. M. D. Bandara and S. C. Burdette, *Chem. Soc. Rev.*, 2012, **41**, 1809.
9   R. Göstl, A. Senf and S. Hecht, *Chem. Soc. Rev.*, 2014, **43**, 1982.
10 W. A. Velema, J. P. van der Berg, M. J. Hansen, W. Zsymanski, A. J. M. Driessen, B. L. Feringa. *Nat. Chem.*, 2013, **5**, 924.
11 R. Lyndon, K. Konstas, B. P. Ladewig, P. D. Southon, C. J. Kepert and M. R. Hill. *Angew. Chem. Int. Ed.*, 2013, **52**, 3695.
12 M. Baroncini and G. Bergamini, *Chemical Record*, 2017, **17**, 700.
13 D.-H. Qu, Q.-C. Wang, Q.-W. Zhang, X. Ma and H. Tian, *Chem. Rev.*, 2015, **115**, 7543.
14 M. Lohse, K. Nowosinski, N. L. Traulsen, A. J. Achazi, L. K. S. von Krbek, B. Paulus, C. A. Schalley and S. Hecht, *Chem. Commun.*, 2015, **51**, 9777.
15 C. Burkhart and G. Haberhauer, *Eur. J. Org. Chem.*, 2017, **10**, 1308.
16 T. Ikegami, Y. Kageyama, K. Obara and S. Takeda, *Angew. Chem. Int. Ed.*, 2016, **55**, 8239.
17 T. Avellini, H. Li, A. Coskun, G. Barin, A. Trabolsi, A. N. Basuray, S. K. Dey, A. Credi, S. Silvi, J. F. Stoddart and M. Venturi, *Angew. Chem. Int. Ed.*, 2012, **51**, 1611.
18 M. Baroncini, C. Gao, V. Carboni, A. Credi, E. Previtera, M. Semeraro, M. Venturi and S. Silvi, *Chem. Eur. J.*, 2014, **20**, 10737.
19 G. Ragazzon, M. Baroncini, S. Silvi, M. Venturi, A. Credi, *Nature Nanotechnology*, 2015, **10**, 70.
20 M. Baroncini, S. Silvi, M. Venturi, A. Credi, *Chem. Eur. J.*, 2010, **16**, 11580.
21 M. Baroncini, S. Silvi, M. Venturi, A. Credi, *Angew. Chem. Int. Ed.*, 2012, **51**, 4223.
22 H. Dürr and H. Bouas-Laurent, in *Photochromism: Molecules and Systems*, Elsevier, Amsterdam, 2003.

23 P. R. Ashton, P. J. Campbell, P. T. Glink, D. Philp, N. Spencer, J. F. Stoddart, E. J. T. Chrystal, S. Menzer, D. J. Williams and P. A. Tasker, *Angew. Chem. Int. Ed.*, 1995, **34**, 1865.

24 P. R. Ashton, R. Ballardini, V. Balzani, M. Gómez-López, S. E. Lawrence, M. V. Martínez-Díaz, M. Montalti, A. Piersanti, L. Prodi, J. F. Stoddart and D. J. Williams, *J. Am. Chem. Soc.*, 1997, **119**, 10641.

25 G. J. E. Davidson, S. J. Loeb, P. Passaniti, S. Silvi, and A. Credi, *Chem. Eur. J.*, 2006, **12**, 3233.

26 J. W. Jones and H. W. Gibson, *J. Am. Chem. Soc.*, 2003, **125**, 7001.

27 S. F. Nelson, R. F. Ismagilov, *J. Phys. Chem. A*, 1999, **103**, 5373.

28 T. Hayashida, H. Kondo, J. Terasawa, K. Kirchner, Y. Sunada and H. Nagashima, *J. Organometallic Chemistry*, 2007, **692**, 382.

29 J. Strakosch, *Ber. Dtsch. Chem. Ges.* 1873, **6**, 1056.

30 C. J. Pedersen, *J. Am. Chem. Soc.* 1969, **89**, 7017.

31 M. Montalti, A. Credi, L. Prodi, M. T. Gandolfi, in *Handbook of Photochemistry – Third Edition,* CRC Press, Boca Raton, 2006.